Neutralizer Hollow Cathode Simulations and Comparisons with Ground Test Data

IEPC-2009-20

Presented at the 31st International Electric Propulsion Conference,
University of Michigan • Ann Arbor, Michigan • USA
September 20 – 24, 2009

Ioannis G. Mikellides,[1] John Steven Snyder,[2] Dan M. Goebel, [3] Ira Katz,[4]
Jet Propulsion Laboratory, California Institute of Technology, Pasadena, CA, 91109

and

Daniel A. Herman[5]
ASRC Aerospace Corporation, Cleveland, OH, 44135

Abstract: The fidelity of electric propulsion physics-based models depends largely on the validity of their predictions over a range of operating conditions and geometries. In general, increased complexity of the physics requires more extensive comparisons with laboratory data to identify the region(s) that lie outside the validity of the model assumptions and to quantify the uncertainties within its range of application. This paper presents numerical simulations of neutralizer hollow cathodes at various operating conditions and orifice sizes. The simulations were performed using a two-dimensional axisymmetric model that solves numerically a relatively extensive system of conservation laws for the partially-ionized gas in these devices. A summary of the comparisons between simulation results and Langmuir-probe measurements is provided. The model has also been employed to provide insight into recent ground test observations of the neutralizer cathode in NASA's Evolutionary Xenon Thruster (NEXT). It is found that a likely cause of the observed keeper voltage drop in long-duration testing is cathode orifice erosion. However, due to the small magnitude of this change, ~0.5 V (<5% of the beginning-of-life value) over 10 khrs, and in light of the large uncertainties of the cathode material sputtering yield at low ion energies, other causes cannot be excluded. Preliminary simulations to understand transition to plume mode suggest that in the range of 3-5 sccm the existing 2-D model reproduces fairly well the rise of the keeper voltage in the NEXT neutralizer as observed in the laboratory. At lower flow rates the simulation produces oscillations in the keeper current and voltage that require prohibitively small time-steps to resolve with the existing algorithms.

I. Introduction

THE Orificed Cathode (OrCa2D) computer code is a two-dimensional (2-D) axisymmetric model of the plasma and neutral gas in electric propulsion (EP) hollow cathodes, and has been developed at JPL to support service life assessment and EP qualification activities for NASA's science missions. The ultimate goal of the life modeling effort is to lower the cost and risk associated with the employment of Solar Electric Propulsion on Discovery, New Frontiers and Flagship missions. The 2-D axisymmetric model simulates the partially-ionized gas that is generated by these devices, both inside the cathode channel (insert region) and outside the channel, around the orifice plate and

[1] Senior Engineer, Electric Propulsion Group, Ioannis.G.Mikellides@jpl.nasa.gov.
[2] Senior Engineer, Electric Propulsion Group, John.S.Snyder@jpl.nasa.gov.
[3] Principal Engineer, Propulsion and Materials Engineering Section, Dan.M.Goebel@jpl.nasa.gov.
[4] Group Supervisor, Electric Propulsion Group, Ira.Katz@jpl.nasa.gov.
[5] Aerospace Engineer, Propulsion and Propellants Branch, Daniel.A.Herman@nasa.gov.

the keeper region. It uses finite volume differencing to solve numerically the multi-species conservation equations for electrons, singly-charged xenon ions and xenon atoms, using a strongly-implicit, time-split approach.

OrCa2D was applied in the past to simulate a variety of discharge hollow cathode (DHC) geometries and operating conditions, and the results have compared well with experimental measurements both inside the device and in the near plume.[1,2] In ring-cusp ion thrusters the DHC typically operates at higher flow rate and total current than the neutralizer hollow cathode (NHC). Moreover, in these engines, the magnetic field supplied by the ring magnets plays no significant role on the evolution of the plasma in the NHC plume. Finally, the current collected by the keeper electrode in a NHC is usually a substantial portion of the total current (beam + keeper current) and the cathode-plate orifice is smaller in diameter compared to a DHC for a given ion engine. These differences combined lead to distinctively different plasma properties in NHCs compared to DHCs that can have important implications on life-limiting mechanisms, such as plume mode, cathode-plate orifice erosion and keeper erosion.

This computational effort was motivated in part by NHC performance results observed during the NEXT Long-Duration Test (LDT). NEXT (NASA's Evolutionary Xenon Thruster) is an advanced ion propulsion system developed by a team led by the NASA Glenn Research Center (GRC) consisting of a 7-kW, 36-cm ion thruster, power processing unit, propellant management system, and gimbal.[3] LDT performance trends over the first 10 khr of operation include a measureable drop in neutralizer keeper voltage that, while not particularly concerning, was not completely understood. Of greater concern was the loss of plume mode flow margin, the difference between the operating flow rate and the flow rate at the transition from "spot mode" to "plume mode," which showed significant changes including negative flow margin at some operating conditions based on the NEXT throttle table.[4,5] The modeling work discussed herein is aimed at understanding these changes and identifying corrective actions.

The paper outline is as follows. A brief description of the 2-D computational model is provided in Section II that includes a synopsis of recent model improvements related to the keeper boundary conditions and plasma resistivity. Section II concludes with a summary of comparisons between numerical simulation results and plasma measurements obtained in the laboratory for various cathode orifice geometries and operating conditions. A more detailed description of these comparisons has been provided in a recent paper by Mikellides, *et al.*[6] Section III presents results from numerical simulations aimed at providing insights into the recent LDT observations. The computed keeper voltage is presented for different cathode orifice shapes that have been prescribed in a manner that emulates the estimated erosion profile. Section III concludes with results from our first numerical simulations of the NEXT NHC at reduced mass flow rates. This first set of simulations is aimed at identifying the physics augmentations needed in OrCa2D to allow for predictions of cathode transition to plume mode.

II. The OrCa2D Computational Model

A. General Description

The features and conservation equations of the two-dimensional computational model OrCa2D used for the NHC plasma simulations has been described in detail in previous articles[7,1] and will only be described briefly here. The model solves the conservation laws for three species present in the partially-ionized gas: electrons, xenon ions and xenon neutrals. It is assumed that only singly-charged ions are present and that the ionized species satisfy quasi-neutrality. The equations of continuity and momentum for ions, and the momentum equation for the electrons, are solved directly to yield the plasma particle density, ion and electron current densities. The combination of the electron and ion continuity equations yields the current conservation law, which is solved implicitly in OrCa2D to obtain the plasma potential. All relevant elastic and inelastic collision frequencies are included in the transport terms. The electron temperature is obtained from the electron energy transport equation, which includes thermal diffusion, energy losses due to ionization and the work done on the electrons by the electric field. The ions and neutrals are assumed to be in thermal equilibrium inside the cathode and a single equation is employed for the conservation of energy of the heavy species. The orifice plate temperature is set equal to the peak emitter temperature. The keeper plate temperature is set at 500 ^{o}C, and although it may deviate from this value depending on the operating condition the results presented herein are not found to be critically sensitive to this boundary condition. Sheath boundary conditions are applied at the cathode wall boundaries that include thermionic electron emission from the emitter. The model requires that the temperature of the emitter be specified. The specification of the emitter temperature requires two inputs: the peak emitter temperature $T_{w,max}$ and a (non-dimensional) polynomial that expresses the variation of the temperature as a function of position along the emitter. The functional form of the fit implemented in the present simulations is based on a measured[8] temperature profile for ¼–in cathode with a 40-mil orifice diameter, and has been presented in Ref. 9.

The neutral gas density is determined by the neutral gas continuity equation and includes the ionization source term for Xe^+. Inside the cathode the neutral gas viscous momentum equations are solved whereas downstream of the cathode orifice a collisionless method is employed to obtain the neutral gas density. The "fluid" and "collisionless" regions are coupled at the transition line, which in the NHC simulations is located at the exit of the cathode orifice's cylindrical section. The numerical approach for the neutral gas fluid momentum equation uses an upwind finite volume scheme by applying first-order upwind fluxes across each edge with no flux-limiting.

The computational region employed for the NHC simulations is illustrated in Figure 1. The computational region employed in the NHC simulations is enclosed by the dashed line. It spans the cathode interior, cathode and keeper orifices, and the cathode's near-plume and far-plume regions. Because the size of the region is limited by the available computational resources an "electrode" boundary is placed far from the cathode to collect the beam current. The computational mesh consists mostly of rectangular cells upstream of the cathode orifice but transitions to a generalized grid arrangement in the plume region. No applied magnetic field is employed in the NHC simulations.

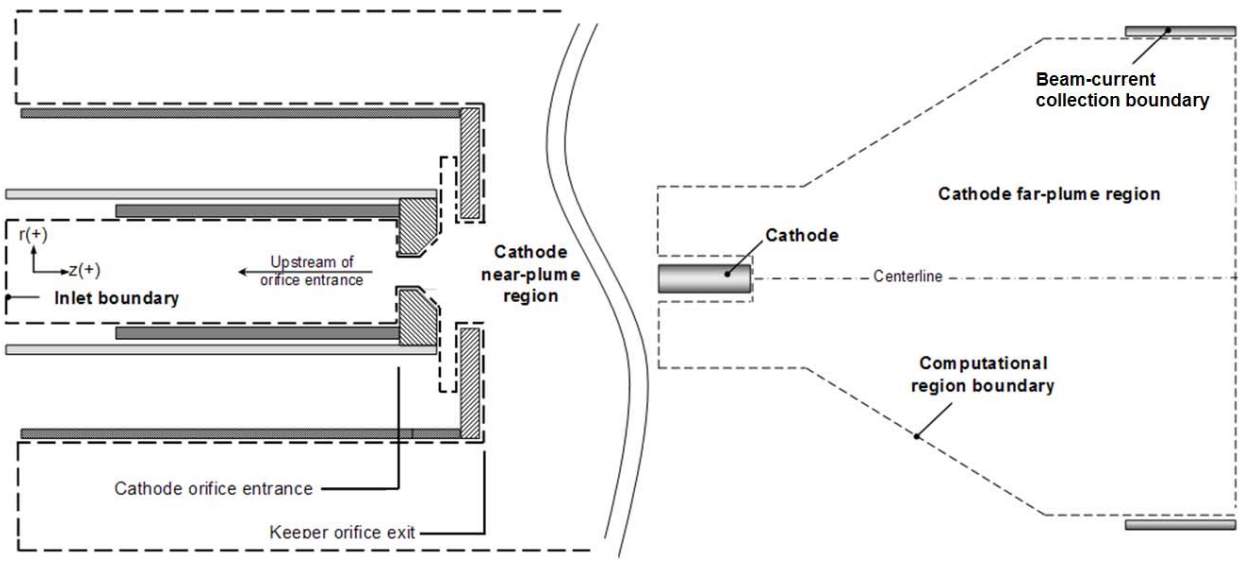

Figure 1. The computational region employed in the NHC simulations is enclosed by the dashed line.

The existing algorithm for the boundary conditions at the keeper electrode allowed for current collection with self-consistent determination of the keeper voltage. The sheath boundary conditions for the electron and ion current densities have been described in Ref. 9. An iterative procedure allows for the determination of V_K based on a prescribed value of the keeper current. In previous simulations, it had been assumed that when the plasma potential $\leq V_K$ the sheath repels all ions and therefore no ion flux to the wall was allowed. Here we find that in the keeper/cathode gap the plasma potential spans the range between the ion-attracting and ion-repelling limits. In this intermediate regime the collected ion flux transitions smoothly from one limit (Bohm) to the other (zero flux). Thus, in the present simulations the model boundary conditions have been modified according to Andrews and Varey[10] who showed that by taking into account the effects of the absorbed electrons a "Bohm reduction factor" may be derived that is dependent upon the sheath drop. In this manner the ion flux is reduced continuously from the ion-attracting to the ion-repelling limits. The formulation and functional form of the reduction factor have been presented in Ref. 9.

A second upgrade of the OrCa2D physics algorithms is related to the collision frequency of the electrons due to wave motion. It has recently been postulated that low-frequency (~100 kHz) turbulence, which has been predicted[11] and measured[12] in the near plume of electric propulsion cathodes, can enhance the collision frequency of the electrons in this region but a functional form of the effective resistivity has been elusive. The difficulty has been largely due to the fact that the saturation of electron-ion streaming instabilities to low-frequency turbulence in these devices is strongly dependent on both the electron drift speed (relative to the ions), which tends to drive the instability, and on collisions with ions,[13,14] neutrals and walls, which tend to damp it. Existing theories that provide

approximate expressions for the collision frequency are based usually on restrictive assumptions such as collisionless and homogeneous plasma none of which applies to the pertinent regions of the cathode plasma. In this work, we have incorporated a non-classical collision frequency in the form of $\nu_a = aKn_e\omega_{pe}$ where "a" is a constant that depends on the orifice geometry, and a numerical value of ~0.4 that we specified based on the guidance of test simulations cases. The classical electron Knudsen number Kn_e is determined based on the density-gradient and the classical electron collision frequencies. In all simulation cases presented here this numerical value has been kept fixed (unless varied for model uncertainty assessments) and therefore the comparisons between theory and experiment have not been controlled by this parameter.

B. Comparisons with Plasma Measurements

Table 1 below lists the different cases we have simulated. The different cases of orifice geometries and operating levels have been chosen to span a relatively wide range of conditions for the ionized gas in these devices. The naming convention we follow for the various cathode cases is a numerical value followed by two letters that identify the operating point as high-power (HP) or low-power (LP). Wherever model inputs (such as the emitter temperature) are unknown, or critical models (such as the numerical value of the effective collision frequency) are uncertain, sensitivity calculations have been performed to quantify such uncertainties. The results of these sensitivity calculations as well as the comparisons for all cases in Table 1 a have been presented in Ref. 7. Here we repeat a few representative cases for completeness.

Table 1. Neutralizer cathode cases simulated with OrCa2D. All geometry related values have been normalized with respect to the 20-HP cathode.

Cathode parameter	20-HP	30-LP	30-HP	40-LP
Cathode tube diameter	1	1	1	1
Emitter length	1	1	1	1
Cathode plate orifice diameter	1	3/2	3/2	2
Keeper plate orifice diameter	1	1	1	1
Keeper plate thickness	1	0.5	0.5	0.5
Cathode-keeper gap	1	1	1	1
Mass flow rate (sccm)	4.0	1.5	3.0	1.5
Discharge voltage, V_d (V)	17.3	23.2	21.0	25.9
Keeper voltage, V_K (V)	12.7	15.25	11.5	12.85
Keeper current, I_K (A)	3.0	1.0	1.0	1.0
Beam current, I_b (A)	3.5	1.5	3.0	1.5

The numerical simulations for all cases were performed using the computational region shown in Figure 1. The computational region employed in the NHC simulations is enclosed by the dashed line, modified for each cathode case only to account for the different cathode orifice size and keeper plate geometry. The data comparisons are performed with simulation results that show small to no variation with numerical simulation time. Depending on the geometry, initial conditions and operating point the numerical simulation time to steady state ranged from a few to several milliseconds. The plasma data ranged from the keeper exit region to several centimeters downstream of the keeper, and were obtained using Langmuir probes in a laboratory vacuum chamber. The overall diagnostics system and test chamber have been described in several previous publications (e.g. see Ref. 15). The background pressure during the tests was in the low values of 10^{-5} Torr. Unless otherwise stated the simulations have assumed a value of 10^{-5} Torr.

The comparison of the plasma potential and electron temperature for the 20-HP cathode are shown in Figure 2. It is found that this cathode exhibits the lowest electron temperature. Operating at the highest mass flow rate and the smallest orifice, this cathode produces the highest plasma (and neutral-gas) densities compared to all other case in Table 1. Thus, the frequency of particle collisions is higher in this cathode, especially inside the orifice, and the contribution to electron heating from wave motion is smaller. That is, the contribution of the effective collision frequency ν_a to the total classical frequency is the smallest by comparison to all the other cathodes. The inclusion of excitation losses in the electron energy law (in addition to the ionization losses already accounted for in all simulations) show negligible differences. All the different simulation cases and comparisons with the measured keeper voltage are listed in Table 2.

Table 2. Description of the various simulation cases and comparisons between the measured and computed keeper voltage (see Figs 9, and 11-15).

Simulation Cases	Keeper Voltage (V_K) Comparison		Reference/Cathode
	Measured (V)	Computed (V) /Simulation case	
(1) Both ionization and excitation losses included – the "nominal simulation case" (solid line) (2) Only ionization losses accounted for in the electron flow (dashed line). The peak emitter temperature for both cases was $T_{w,max}$=950 °C	12.7	12.8 / (1)	Figure 2/20-HP
(1) $T_{w,max}$=950 °C (solid line) (2) $T_{w,max}$=1000 °C (dashed line)	11.5	12.1 / (1) 11.25 / (2)	Figure 3/30-HP
(1) Numerical value of effective collision frequency coefficient a=0.4 (thick line) (2) Numerical value of effective collision frequency coefficient a=0.2 (thin line)	12.85	11.5 / (1) 11.4 / (2)	Figure 4 (right)/40-LP

The comparisons for the 30-HP and 40-LP cathodes are shown in Figures 3 and 4, respectively. The simulation results show elevated electron temperatures by comparison to the 20-HP cathode. We find this to be due to a larger contribution of the non-classical collision frequency ν_a to the heating of the electrons. The largest discrepancy between theory and experiment is observed in the 40-HP where the LP operating condition for the given orifice size has excited strong plasma oscillations by comparison to the 30-XX, as shown in Figure 4 (left). Thus our uncertainty on the numerical value of the constant "a" is the largest for this case. A sensitivity calculation compares the simulation result in Figure 4 (right) for a=0.2 and a=0.4.

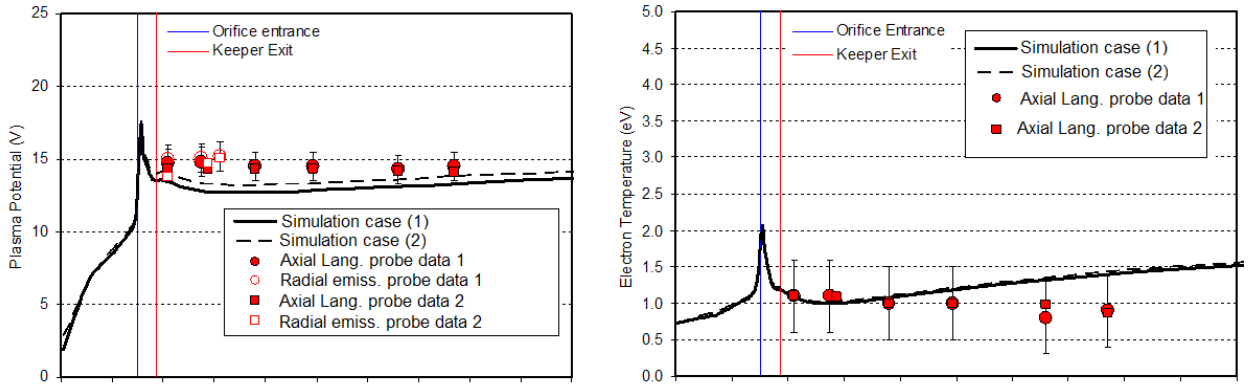

Figure 2. Comparisons for the 20-HP cathode. The peak emitter temperature for both simulation cases was $T_{w,max}$=950 °C.

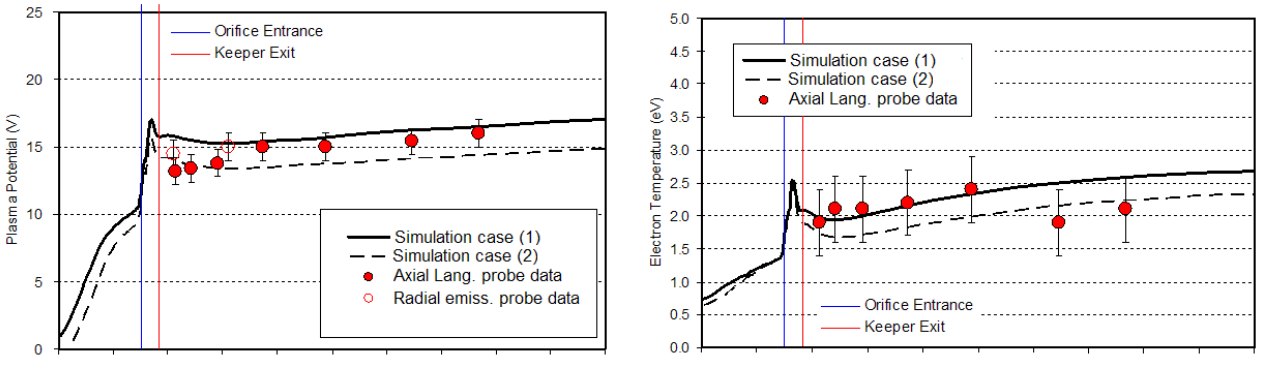

Figure 3. Comparisons and sensitivity of simulation results on uncertain model inputs for the 30-HP cathode.

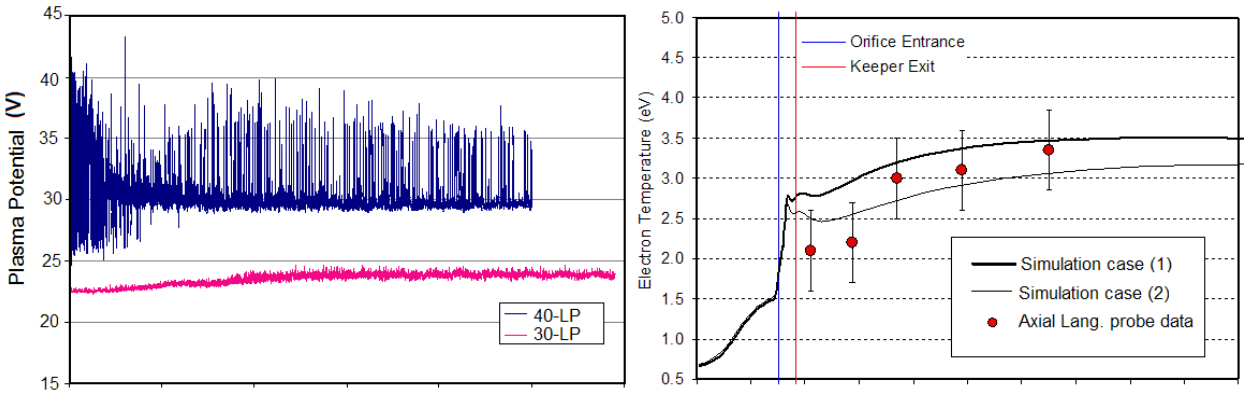

Figure 4. Plasma potential fluctuations as a function of radial position from the axis of symmetry, measured 3 mm downstream of the keeper in 30-LP and 40-LP cathodes. Right: Comparisons and sensitivity of simulation results on uncertain model inputs for the 40-LP cathode along the axis of symmetry ($T_{w,max}$=1050 ^{o}C for both cases).

Because the plasma density falls by several orders of magnitude in the plume region of these devices probe collection spans in all cases presented here both the thin-sheath and Orbit Motion Limited (OML) regimes. Thus, probes of different geometries have been used, and the methods to analyze the data at the two different limits have been based on well-known probe theories. A comparison between the simulation results and the density data was presented in Ref. 6. The largest uncertainty in the plasma density comparisons was found to be in the intermediate regime between the thin-sheath and OML limits, which lies a few keeper diameters downstream keeper exit for the 20-HP. Nearer the keeper electrode where the importance of model predictions becomes more critical the comparison is improved; for example, inside the keeper orifice the discrepancy was found to be less than 17%. The model inside the cathode has remained largely unchanged since the early development of OrCa2D and the agreement with density data in these regions has been within the experimental uncertainty.[16,17]

III. Insights into Ground Test Observations

LDT performance trends over the first 10 khr of operation of NEXT revealed a slow reduction of the neutralizer keeper voltage. The largest drop, about 0.4 V, occurred in less than 6000 hrs. The trend, while not particularly concerning, was not completely understood. Of greater concern was the loss of plume mode flow margin, which showed significant changes including negative flow margin based on Throttle Table 9 (TT9) values. It is noted that TT9 was the baseline table at the beginning of the LDT; to ensure adequate flow margin a new table, TT10, has been released.[4] After 24,400 hrs, in-situ images of the neutralizer cathode plate show no erosion of the orifice minimum diameter but a ~20% increase of the maximum chamfer diameter.[4]

In this section we describe results from modeling studies aimed at addressing both these trends. First, we show that erosion of the NHC orifice is a probable cause of the keeper voltage drop. However, due to the extremely slow rate with which this has occurred in the LDT (~0.5×10^{-4} V/hr), and due to the large uncertainties in the erosion predictions that are mainly due to the lack of sputtering yield data at the energy range of ions bombarding the cathode orifice, other causes cannot be ruled out. In regards to plume mode we present our first results from numerical simulations at reduced cathode flow rates and discuss the computed response of the keeper voltage by comparison with test data.

A. Keeper Voltage and Orifice Erosion

A major challenge in cathode orifice erosion predictions is related to the low energies with which ions strike the surfaces in this area of the cathode. Figure 5 (left) shows computed plasma potential contours of the simulated NEXT NHC. The result suggests that if the ions gain the energy with which they strike the surface as a result of their acceleration through the sheath then this energy (per charge) ranges ~10-14 V. For tungsten (W) no sputtering yield (Y) data exist in this range (Figure 5, right) so erosion predictions must rely on extrapolated fits. In the present set of erosion simulations we have updated a previous extrapolation of the W-yield fit to low energies using the observed erosion of the NSTAR neutralizer cathode at the orifice entrance after two long duration ion engine tests.[18,19] Specifically, to obtain a better estimate of the sputtering yield at low ion energies (ε_i/e<12 V) we have calibrated our

previous simulations[20] of the NSTAR NHC orifice erosion with the observed value at the orifice entrance. That is, we use a single point, namely the observed erosion at the orifice entrance of the NSTAR NHC and iterate until we find the value of the sputtering yield that produces the observed erosion at that point. The computed ion energy at this location is ~11 V.[20] The new sputtering yield value at this energy allowed us to produce the new W-yield fit given by Eq. (1) and plotted in Figure 5 (right). This new fit has been used to compute a new profile for the NSTAR NHC (Figure 6), and it is used here also to estimate the erosion profile in the NEXT NHC (Figure 5, left). This is done by multiplying the computed erosion rate by 3 khrs, approximately the midpoint between the start of the test and the time (~6 khrs) by which most of the voltage drop was observed; based on in-situ images, it is also about this time that erosion of the orifice chamfer appeared to subside.[4] We note that the true erosion is likely less than that shown in Figure 5 since the erosion rate is reduced as the orifice opens because both the ion density (see Figure 7) and the plasma potential decrease with larger orifice area (with everything else being fixed).

$$Y(\bar{\varepsilon}_i) = \exp\left[-30.192 - 84.137\exp(-0.275\bar{\varepsilon}_i) + 5.61\ell n(\bar{\varepsilon}_i)\right] \quad \bar{\varepsilon}_i = \varepsilon_i / e \tag{1}$$

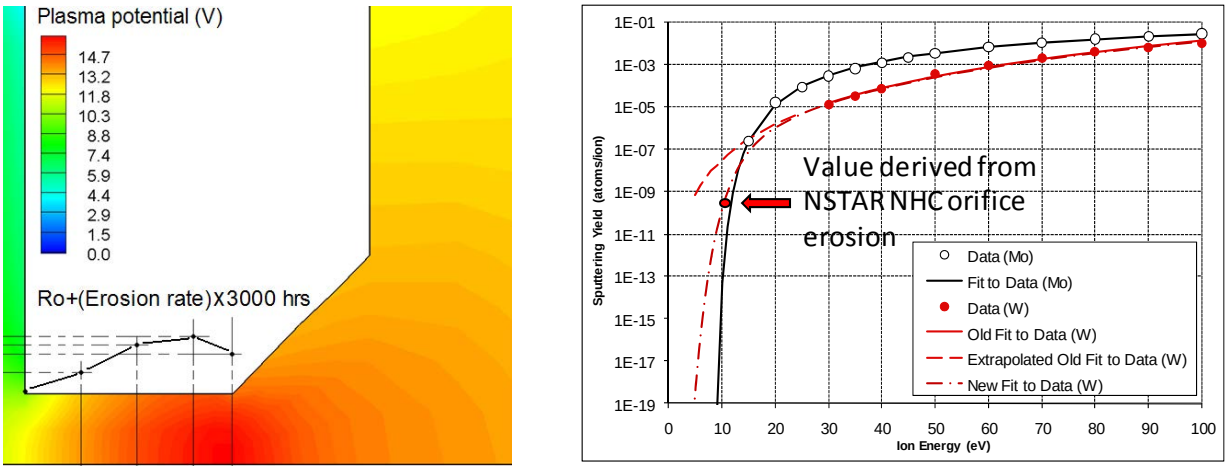

Figure 5. Left: Computed plasma potential contours and estimated orifice erosion profile. Right: Sputtering yield data and extrapolation fits used in the erosion calculations. (Ro is the radius of the cylindrical section of the orifice at beginning of life).

To assess the effect of orifice erosion on the keeper voltage we have used the erosion profile of Figure 5 (left) to guide the construction of two new computational regions of the cathode orifice that emulate an eroded surface as shown by "erosion 1" and "erosion 2" in Figure 8 (right). The goal is to find whether the opening of the NHC orifice to profiles comparable to what is expected (based on the current observations in the LDT and on the numerical simulation result in Figure 5) affects the keeper voltage in the manner observed during the LDT. If yes, then this would warrant more computationally intense simulations that self-consistently compute erosion and keeper voltage as a function of operation time. We find that erosion profiles 1 and 2 (Figure 8, right) produce both the observed trend and the observed magnitude of reduction within a factor of two (0.2 V versus ~0.4 V) as shown in Figure 8 (left).

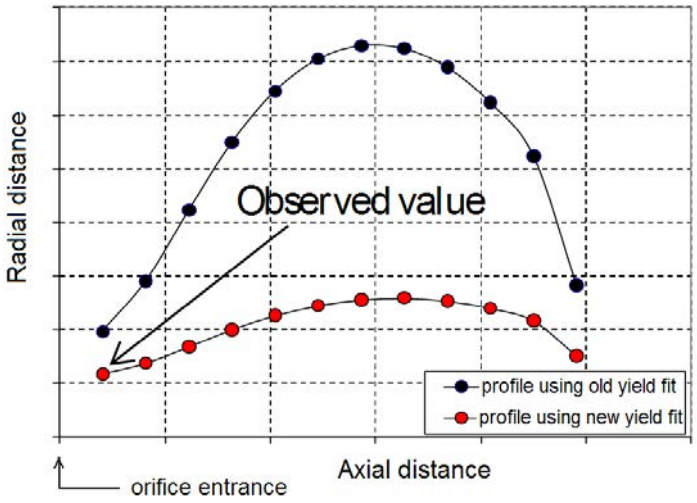

Figure 6. Erosion profiles in the orifice of NSTAR neutralizer cathode. The observed value of the erosion at the orifice entrance after two long-duration tests has been combined with existing numerical simulation of this cathode to obtain a new extrapolation fit for the sputtering yield of tungsten in the range of ion energies for which data do not exist.

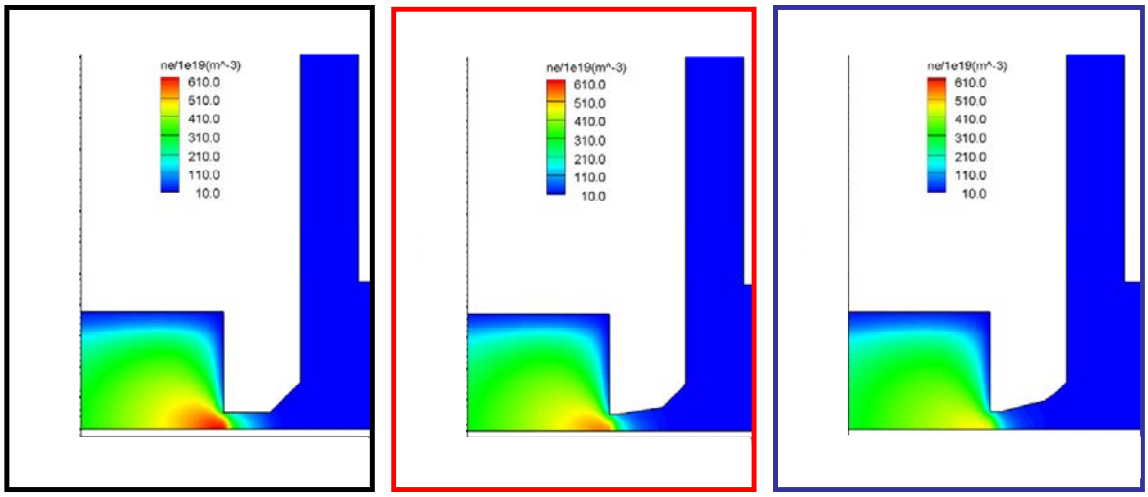

Figure 7. Contours of electron number density in the NEXT NHC as computed by OrCa2D for no erosion of the orifice (left), erosion profile #1 (middle) and erosion profile #2 (right).

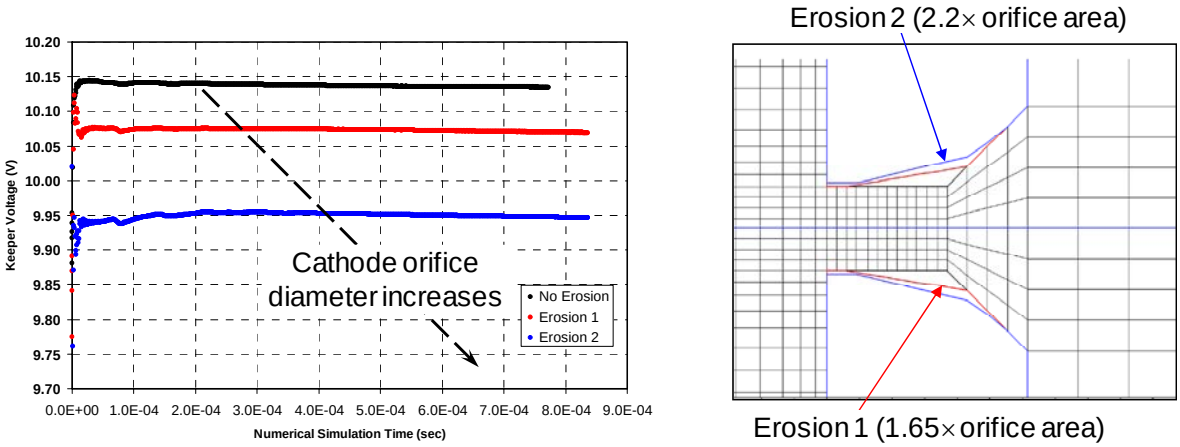

Figure 8. Computed keeper voltage as a function of time (left) for three different configuration of the NEXT neutralizer cathode orifice (right). The results show a decrease of the keeper voltage as the orifice is enlarged by erosion. For the prescribed erosion profiles the computed decrease is ~0.2 V.

B. Preliminary Studies of Transition to Plume Mode

The favorable comparisons in Section II.B between the NHC model results and the plasma measurements in spot-mode operation has motivated a first series of simulations of operating conditions that force the cathode to transition to plume mode. The results of these simulations are presented in this section. The physics that drive the cathode to plume mode are not yet understood and, to the best of our knowledge, there is no physics-based model in existence that predicts spot-to-plume mode transition. Our approach here is to employ the existing NHC model to simulate low cathode flow rates and allow the results to guide augmentations of the physics models as deemed necessary.

For most typical cathodes in electric propulsion, transition to plume mode will occur when the flow rate through the cathode is reduced, at fixed beam and keeper currents. This "transition" is manifested by an increase of the peak-to-peak amplitudes and time-averaged values of the keeper voltage. A typical trend obtained during a laboratory test of the NEXT NHC is shown in Figure 9 (bottom).

The numerical simulations of this cathode held all operational specifications the same as for the nominal case (4 sccm case), including the peak emitter temperature (950 ^{o}C), and varied only the mass flow rate. The results at three flow rates, 3, 4 and 5 sccm show an increase in the keeper voltage with reduced flow rates but at a slightly higher rate compared to the observation. Polk *et al.*[8] have shown by measurements in a similar cathode with a 30-mil-diameter orifice that the peak emitter temperature increased by several degrees as the flow rate was reduced at fixed

discharge current. By iteration between the computed keeper voltage and the specified peak emitter temperature during the numerical simulations of the NEXT NHC we find that at 3 sccm, where the original simulations over-predicted the observed keeper voltage by a few tenths of a volt, a 25 ^{o}C increase in the emitter temperature would be sufficient to account for the discrepancy. This is shown in Figure 9 by the filled rectangular symbol associated with $T_{w,max}$=975 ^{o}C. All simulations down to 3 sccm produced a steady-state solution. A representative history plot of the keeper voltage and current as functions of numerical simulation time is shown in Figure 9, top-right. Further reduction of the flow rate to a value of 2 sccm produces noticeable oscillations in the numerical solution when the same time step is used. The temporal analysis of the observed fluctuations in the numerical simulations is currently underway.

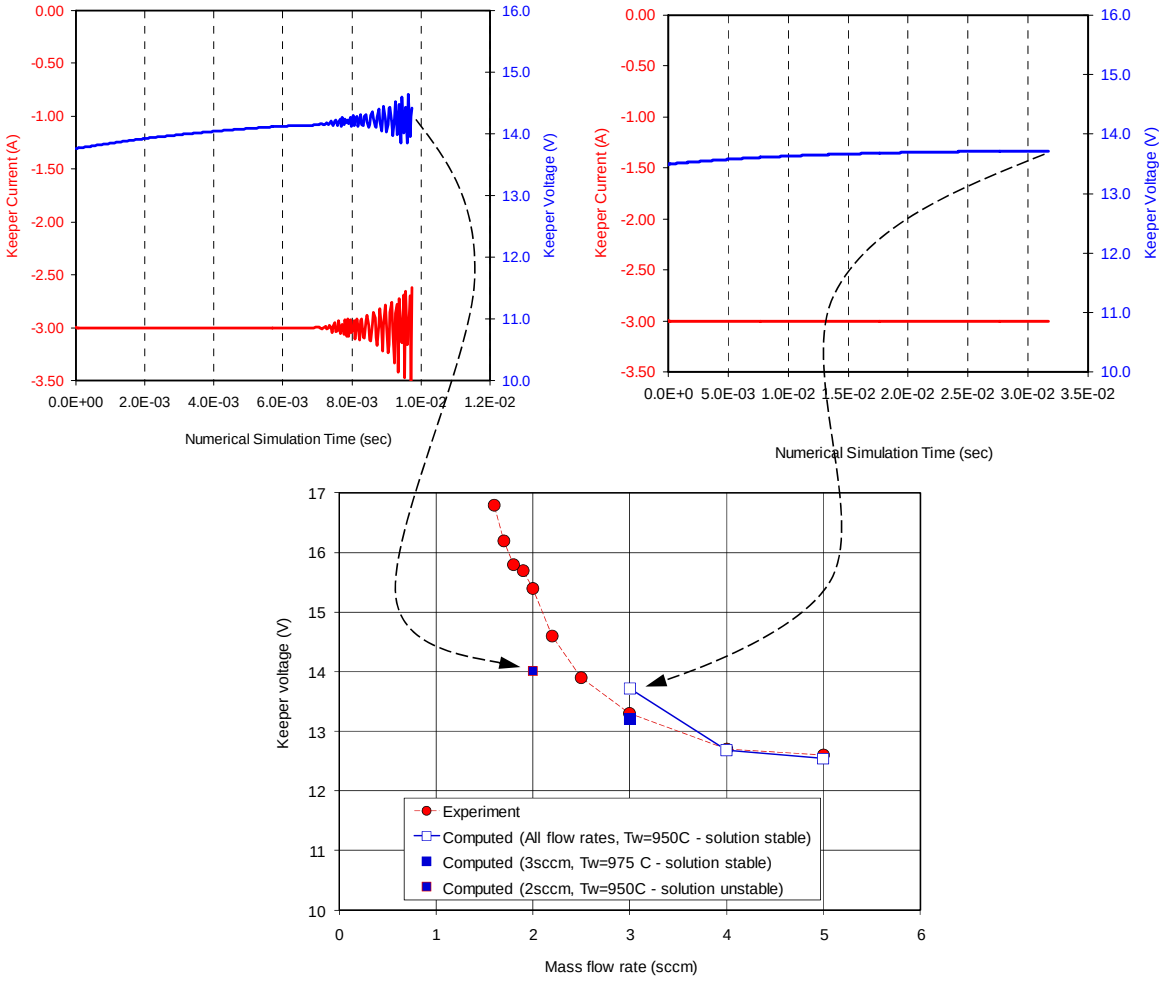

Figure 9. Top: Evolution of keeper voltage and current during the numerical simulation. Bottom: Experiment versus OrCa2D predictions (at $T_{w,max}$=975 ^{o}C) of the keeper voltage as a function of mass flow rate. A sensitivity case for $T_{w,max}$=975 ^{o}C is also included at 3 sccm.

IV. Conclusion

This paper summarized results from the validation simulations OrCa2D, a two-dimensional computer code that solves numerically an extensive system of conservation laws for the partially-ionized gas in hollow cathodes. Results for the plasma potential and electron temperature compare favorably with laboratory measurements when the cathode is operated in spot mode. The computed values for the keeper voltage also compare well with the values recorded during the experiments. The different cathode cases chosen for the simulations and tests were intentionally selected to span a relatively wide operation range for EP neutralizers. The broad objective has been to identify the validity range of the OrCa2D model as well as operation regimes of increased uncertainty. It is found that for all

cases examined here, the model predictions are close to or within the uncertainty of the plasma data. The largest uncertainty in the model results is associated with the model of non-classical collision frequency. Thus, the uncertainty in our predictions decreases with increasing mass flow rate and decreasing cathode orifice diameter; this is because for these neutralizers the contributions of the non-classical frequency to the model results are reduced. For a given operating current, as the flow rate is reduced and/or the orifice is enlarged the cathode moves toward plume mode and the uncertainty in the (spot-mode) model predictions increases.

A more near-term goal has been to provide insight into recent observations in an ongoing wear test of NEXT. In regards to the drop of the neutralizer keeper voltage we find orifice erosion to be the probable cause. However, in light of the large uncertainties of the sputtering yield at low ion energies and the small value of the total voltage drop (<0.5 V occurring over thousands of hours), other causes cannot be ruled out. In regards to plume mode, based on a first set of simulations, we find that OrCa2D re-produces fairly well the rise of the keeper voltage in the range 3-5 sccm. But the limited range of simulation cases attempted so far must be substantially extended before detailed insight into plume-mode physics can be provided.

Acknowledgments

The research described in this paper was carried out by the Jet Propulsion Laboratory, California Institute of Technology, under a contract with the National Aeronautics and Space Administration. Reference herein to any specific commercial product, process, or service by trade name, trademark, manufacturer, or otherwise, does not constitute or imply its endorsement by the United States Government or the Jet Propulsion Laboratory, California Institute of Technology. Portions of the work described herein were funded by NASA's In-Space Propulsion Technology Program under the NEXT Project, led by the NASA Glenn Research Center, with Scott Benson as the Project Manager and Mike Patterson as the Principal Investigator.

V. References

[1] Mikellides, I. G., Katz, I., Goebel, D. M., Jameson, K. K., and Polk, J. E., "Wear Mechanisms in Electron Sources for Ion Propulsion, II: Discharge Hollow Cathode," *J. Prop. Power*, Vol. 24, No. 4, 2008, pp. 866-879.
[2] Mikellides, I. G., Katz, I., Goebel, D. M., and Polk, J. E., "Assessments of Hollow Cathode Wear in the Xenon Ion Propulsion System (XIPS©) by Numerical Analyses and Short-Duration Tests," AIAA Paper 08-5208, July 2008.
[3] Patterson, M.J., and Benson, S.W., "NEXT Ion Propulsion System Development Status and Performance," AIAA Paper 07-5199, July 2007.
[4] Herman, D. A., Soulas, G. C., and Patterson, M. J., "NEXT Long-Duration Test Neutralizer Performance and Erosion Characteristics," IEPC Paper 09-154, September 2009.
[5] Herman, D.A., Soulas, G. C., and Patterson, M. J., "Performance Characteristics of the NEXT Long-Duration Test after 16,550 h and 337 kg of Xenon Processed," AIAA Paper 08-4527, July 2008.
[6] Mikellides, I. G., Goebel, D. M., Snyder, J. S., Katz, I. and Herman, D. H., "Neutralizer Hollow Cathode Simulations, Validation with Experiments," AIAA Paper 09-5196, July 2009.
[7] Mikellides, I. G., and Katz, I., "Wear Mechanisms in Electron Sources for Ion Propulsion, I: Neutralizer Hollow Cathode," *J. Prop. Power*, Vol. 24, No. 4, 2008, pp. 855-865.
[8] Polk, J. E., Marrese, C., Thornber, B., Dang, L., and Johnson, L., "Temperature Distributions in Hollow Cathode Emitters," AIAA Paper 04-4116, July 2004.
[9] Mikellides, I. G., Goebel, D. M., Snyder, J. S., and Herman, D. A., "Neutralizer Hollow Cathode Simulations and Validation with Experiments," AIAA Paper 09-5196, July 2009.
[10] Andrews, J. G., And Varey, R. H., "The Sheath at an Electrode Close to Plasma Potential," *J. Phys. A: Gen. Phys.*, 1970, Vol. 3, pp. 413-420.
[11] Mikellides, I. G., Katz, I., Goebel, D. M., and Polk, J. E., "Hollow Cathode Theory and Experiment, II. A Two-Dimensional Theoretical Model of the Emitter Region," *J. Appl. Phys.*, Vol. 98, No. 11, 2005, pp. 113303 (1-14).
[12] Goebel, D. M., Jameson, K. K., Katz, I., and Mikellides, I. G., "Energetic Ion Production and Electrode Erosion in Hollow Cathode Discharges," IEPC Paper 2005-266, October 2005.
[13] Epperlein, E. M., Short, R. W., and Simon, A. "Damping of Ion-Acoustic Waves in the Presence of Electron-Ion Collisions," *Phys. Rev. Letters*, Vol. 69, No. 12, 1992, pp. 1765-1768.
[14] Maksimov, A. V., and Silin, V. P., "Damping of Ion Acoustic Waves in a Plasma with Rare Collisions in Connection with Nonlocal Hydrodynamics," *JETP Lett.*, Vol. 59, No. 8, 1994, pp. 534-536.

[15] Goebel, D. M., Jameson, K. K., Watkins, R. M., Katz, I., and Mikellides, I. G., "Hollow Cathode Theory and Experiment, I. Plasma Characterization Using Fast Miniature Scanning Probes," *J. Appl. Phys.*, Vol. 98, No. 11, 2005, pp. 113302 (1-9).
[16] Mikellides, I. G., "Effects of Viscosity in a Partially Ionized Channel Flow with Thermionic Emission," *Phys. Plas.*, Vol. 16, 013501, 2009.
[17] Mikellides, I. G., Katz, I., Goebel, D. M., and Jameson, K. K., "Evidence of Nonclassical Plasma Transport in Hollow Cathodes for Electric Propulsion," *J. Appl. Phys.*, Vol. 101, 063301, 2007.
[18] Polk, J. E., Anderson, J. R., Brophy, J. R., Rawlin, V. K., Patterson, M. J., Sovey, J., and Hamley, J., "An Overview of the Results from an 8200 Hour Wear Test of the NSTAR Ion Thruster," AIAA Paper 99-2446, June 1999.
[19] Sengupta, A., Brophy, J. R., and Goodfellow, K. D., "Status of the Extended Life Test of the Deep Space 1 Flight Spare Ion Engine after 30,352 Hours of Operation," AIAA Paper 03-4558, July 2003.
[20] Mikellides, I. G., and Katz, I., "The Partially-Ionized Gas and Associated Wear in Electron Sources for Ion Propulsion, I: Neutralizer Hollow Cathode," *J. Prop. Power*, Vol. 24, No. 4, 2008, pp. 855-865.